Quality Improvement Study

INTERNATIONAL JOURNAL OF SURGERY

OPEN

Design of well-matched end-structure of anatomical proximal femoral locking plate based on computer-assisted imaging combined with 3D printing technology: a quality improvement study

Xiaoyang Jia, MD, PhD[a], Kun Zhang, MD, PhD[b], Minfei Qiang, MD, PhD[c], Qinghui Han, MD[b], Guojun Zhao, MD[d], Ying Wu, MD, PhD[e], Yanxi Chen, MD, PhD[c,*]

Background: The extramedullary locking plate system was the common internal fixation method for hip fractures. However, common plates were poorly matched to femur, which was because they were designed based on anatomical parameters of the Western populations. Therefore, the aim was to design an end-structure of the anatomical proximal femoral locking plate that closely matched the anatomy of the Chinese population.

Materials and methods: From January 2010 to December 2021, consecutive patients aged 18 years and older who underwent a full-length computed tomography scan of the femur were included. The end-structure (male and female model) of the anatomical proximal femoral locking plate was designed based on anatomical parameters of femurs that were measured in three-dimensional space using computer-assisted virtual technology. The match degree between the end-structure and femur were evaluated. Inter-observer and intra-observer agreement for the evaluation of match degree was assessed. The matching evaluation based on a three-dimensional printing model was regarded as the gold standard to assess the reliability.

Results: A total of 1672 patients were included, with 701 men and 971 women. Significant differences were seen between male and female for all parameters of the proximal femur (all $P < 0.001$). All match degree of end-structure was over 90%. Inter-observer and intra-observer agreement was almost perfect (all kappa value, > 0.81). The sensitivity, specificity, and percentage of correct interpretation of matching evaluation in the computer-assisted virtual model was all greater than 95%. From femur reconstruction to completion of internal fixation matching, the process takes about 3 min. Moreover, reconstruction, measurement, and matching were all completed in one system.

Conclusions: The results showed that based on the larger sample of femoral anatomical parameters, a highly matching end-structure of anatomical proximal femoral locking plate for Chinese population could be designed with use of computer-assisted imaging technology.

Keywords: 3D printing, computer-assisted technology, hip fractures, internal fixation design, match, proximal femoral fractures

Introduction

With rapid urbanization, motorization, and an aging population, the incidence of injury-related fractures is also increasing[1,2]. Hip fractures are the most common type of fracture encountered, disabling 4.5 million people worldwide each year. The number of people who will be living with disabilities is expected to increase

[a]Department of Orthopedic Surgery, Changzheng Hospital, Naval Medical University (Second Military Medical University), [b]Department of Orthopedic Trauma, East Hospital, Tongji University School of Medicine, [c]Department of Orthopedic Surgery, Zhongshan Hospital, Fudan University, Shanghai, [d]Walkman biomaterial CO., LTD, Tianjin and [e]Department of Biostatistics, Guangdong Provincial Key Laboratory of Tropical Disease Research, School of Public Health, Southern Medical University, Guangdong, Guangzhou, China

Xiaoyang Jia, Kun Zhang, and Minfei Qiang contributed equally to this article.

Sponsorships or competing interests that may be relevant to content are disclosed at the end of this article.

*Corresponding author. Address: Department of Orthopedic Surgery, Zhongshan Hospital, Fudan University, 180 Fenglin Rd, Shanghai 200032, China. Tel: +86 216 404 1990, fax: +86 216 277 8076. E-mail: cyxtongji@126.com (Y Chen).

International Journal of Surgery (2023) 109:1169–1179

Received 18 October 2022; Accepted 13 February 2023

Supplemental Digital Content is available for this article. Direct URL citations are provided in the HTML and PDF versions of this article on the journal's website, www.journal-surgery.net.

Published online 10 April 2023

http://dx.doi.org/10.1097/JS9.0000000000000300

to 21 million in the next 40 years[3–6], which introduces new health challenges to trauma surgeons[7].

The natural history of hip fractures is dismal if left untreated. Therefore, timely surgery remains the mainstay treatment[8]. With the development of internal fixation devices, extramedullary systems have become a common method for fixation of hip fractures, particularly the locking plate system[8–11]. From a biomechanical viewpoint, an appropriately contoured plate is crucial to establish a strong bone-plate construction for fracture stabilization, even with a locking compression plate[12,13]. However, the current extramedullary plates do not match the proximal femur contour, making it difficult to place the plate in the optimal position[13–15]. This increases the number of intraoperative plate adjustments, operative time, and intraoperative blood loss; a mispositioned plate has an altered biomechanical behavior and weakens the mechanical stability of the injured bone[16]. A poor match between the plate and the lateral femoral edge is prone to large gaps, resulting in postoperative complications such as congestion and infection.

The mismatch between the plate and proximal femur may originate from the following points: First, most femoral locking plate systems are designed based on anatomical parameters of the Western population[17,18], which significantly differ between races[14,18,19]. Second, the traditional design of internal fixation devices is primarily based on the morphological parameters of cadavers. Cadaveric sample sizes are extremely limited, which leads to the measured parameters being unrepresentative. Finally, the anatomy of the proximal femur is complex, which causes considerable difficulties in designing an ideal internal fixation device.

No well-matched proximal femoral locking plate systems have been designed based on the anatomical parameters of the Chinese population. Therefore, the aim of this study was to design an end-structure of the anatomical proximal femoral locking plate that closely matched the anatomy of the Chinese population based on an artificial intelligence image-fusion platform and a large database, using computer-assisted imaging and three-dimensional (3D) printing technology. Additionally, the purpose was to develop an efficient and economical design process for internal fixation systems, which can be used as a valuable reference in the future. The hypothesis was that a well-matched end-structure of the anatomical proximal femoral locking plate could be designed by accurately measuring the anatomical parameters of the proximal femur.

HIGHLIGHTS

- End-structure design is based on the anatomical parameters of 1672 femurs.
- The match between the end-structure and proximal femur is very good.
- The good match between the end-structure and proximal femur is verified on the three-dimensional printing model.
- The design process for the internal fixation system is efficient and economical, which is valuable experience for future reference.

Materials and methods

Data sources

This study was approved by the Institutional Review Board. The need for informed consent was waived because deidentified data was used. This study was conducted using the hospital information and imaging systems, which contain patient demographics and imaging data from both the outpatient and inpatient settings. This work was reported in accordance with SQUIRE 2.0 Criteria[20], Supplemental Digital Content 1, http://links.lww.com/JS9/A245.

Study population

Consecutive patients aged 18 years and older who underwent a full-length computed tomography (CT) scan of the femur from 1 January 1 2010, to 31 December 31 2021 were included (1773 patients; 748 males and 1025 female). Patients with femoral deformities, hip osteoarthritis, femoral fractures, previous hip surgery, or a history of femoral trauma were excluded. Two experienced orthopedic surgeons reviewed all the CT scans to confirm that each patient met the inclusion and exclusion criteria.

3D model reconstruction

The thin-slice CT axial images of all femurs from a 16- or 32-detector spiral CT scanner (GE LightSpeed; GE Medical Systems) were imported into a computer-assisted orthopedic clinical research platform (SuperImage system, orthopedic edition 1.1; Cybermed)[21,22]. A 3D image of the femur was reconstructed using a surface-shaded display algorithm with a reconstruction interval of 0.625 mm (Fig. 1A, B). In the 3D surface-shaded display images, component bones were distinguished using an interactive automatic segmentation technique. Different bones were labeled with distinct colors, and the femur was generated after removing unrelated bones.

Parameter measurements

Relevant points, lines, and planes were defined to measure anatomical parameters of the proximal femur (SFig. 1, Supplemental Digital Content 2, http://links.lww.com/JS9/A246, SFig. 2, Supplemental Digital Content 2, http://links.lww.com/JS9/A246, and SFig. 3, Supplemental Digital Content 2, http://links.lww.com/JS9/A246). The length of the long axis of the femoral neck was defined as the distance between the two intersections of the femoral head and the lateral wall of the femur along the central axis of the femoral neck (Fig. 1A). The neck-shaft angle was the angle between the central axes of the femoral neck and femoral shaft (Fig. 1A)[23]. Anteversion of the femoral neck was derived by determining the angle between the transcondylar plane and the plane constructed by the intersection of the axes of the femoral neck and shaft (Fig. 1B)[23]. The height of the lateral femoral wall was defined as the vertical distance from the lateral femoral muscle crest to the level of the lesser trochanter (Fig. 1C). The width of the lateral femoral wall was defined as the anteroposterior diameter of the femoral muscle crest on the lateral wall (Fig. 1D). The superior radius of the lateral femoral wall was defined as the radius of the best-fit circle at the lateral facet of the greater

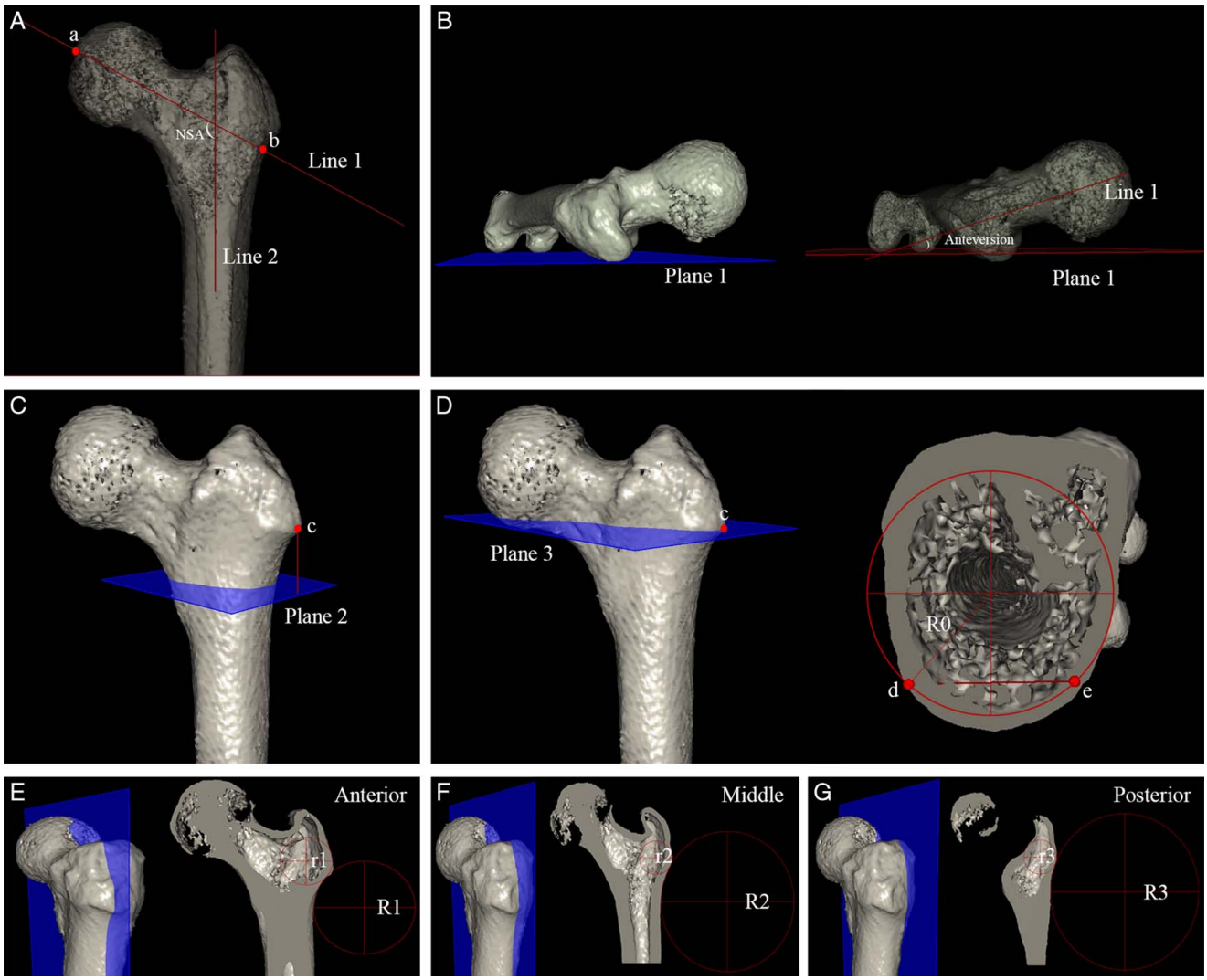

Figure 1. Anatomical parameters of the proximal femur. (A) Length of long axis of the femoral neck was the distance from point a to point b; point a, the intersection of femoral head and central axis of the femoral neck (line 1); point b, the intersection of lateral wall and central axis of the femoral neck (line 1). Neck-shaft angel was the angle between the central axis of the femoral neck (line 1) and the long axis the femoral shaft (line 2). (B) Anteversion of femoral neck was derived from determining the angle between the transcondylar plane (plane 1) and the central axis of the femoral neck (line 1). (C) Height of the lateral femoral wall was the vertical distance from the lateral femoral muscle crest (point c) to the level of the lesser trochanter (plane 2). (D) Width of the lateral femoral wall was the distance from point d to point e; point d and point e, intersection of the horizontal plane of the femoral muscle crest on the cortex of the lateral wall. Radian of the lateral femoral wall (R0) was the radius of a best-fit circle of the cross section of the lateral femoral muscle crest on the lateral femoral wall. (E, F, and G) Superior radius of lateral femoral wall was the radius of a best-fit circle on the lateral facet of the greater trochanter, which was divided into anterior (r1), middle (r2), and posterior (r3) section. Inferior radius of lateral femoral wall was the radius of a best-fit circle on the distal border of the greater trochanter, which was divided into anterior (R1), middle (R2), and posterior (R3) section.

trochanter (Fig. 1E–G). The inferior radius of the lateral femoral wall was defined as the radius of the best-fit circle at the distal border of the greater trochanter (Fig. 1E–G). The superior and inferior radii were divided into anterior, middle, and posterior sections. The radian of the lateral femoral wall was defined as the radius of the best-fit circle of the cross section of the lateral femoral muscle crest (Fig. 1D).

Definition of end-structure matching

The first versions of the end-structure were designed based on the anatomical parameters of the femur, and were divided into four models based on the differences in skeletal morphology between males and females (male, left and right; female, left and right) (Fig. 2)[13,24]. The left and right models were mirror structures. The matching of the end-structure and proximal femur was evaluated using the computer-assisted orthopedic clinical research platform (Fig. 3). Six gaps between the end-structure and plate were identified as indicators and were measured (Fig. 4). The gaps were as follows: superior and inferior arcs anteriorly (Fig. 4A); superior and inferior arcs posteriorly (Fig. 4B); proximal end (Fig. 4C); and distal end (Fig. 4D). If the gap was less than or equal to 2 mm, it was allotted 1 point. A total score of greater than or equal to 4 was considered a good match.

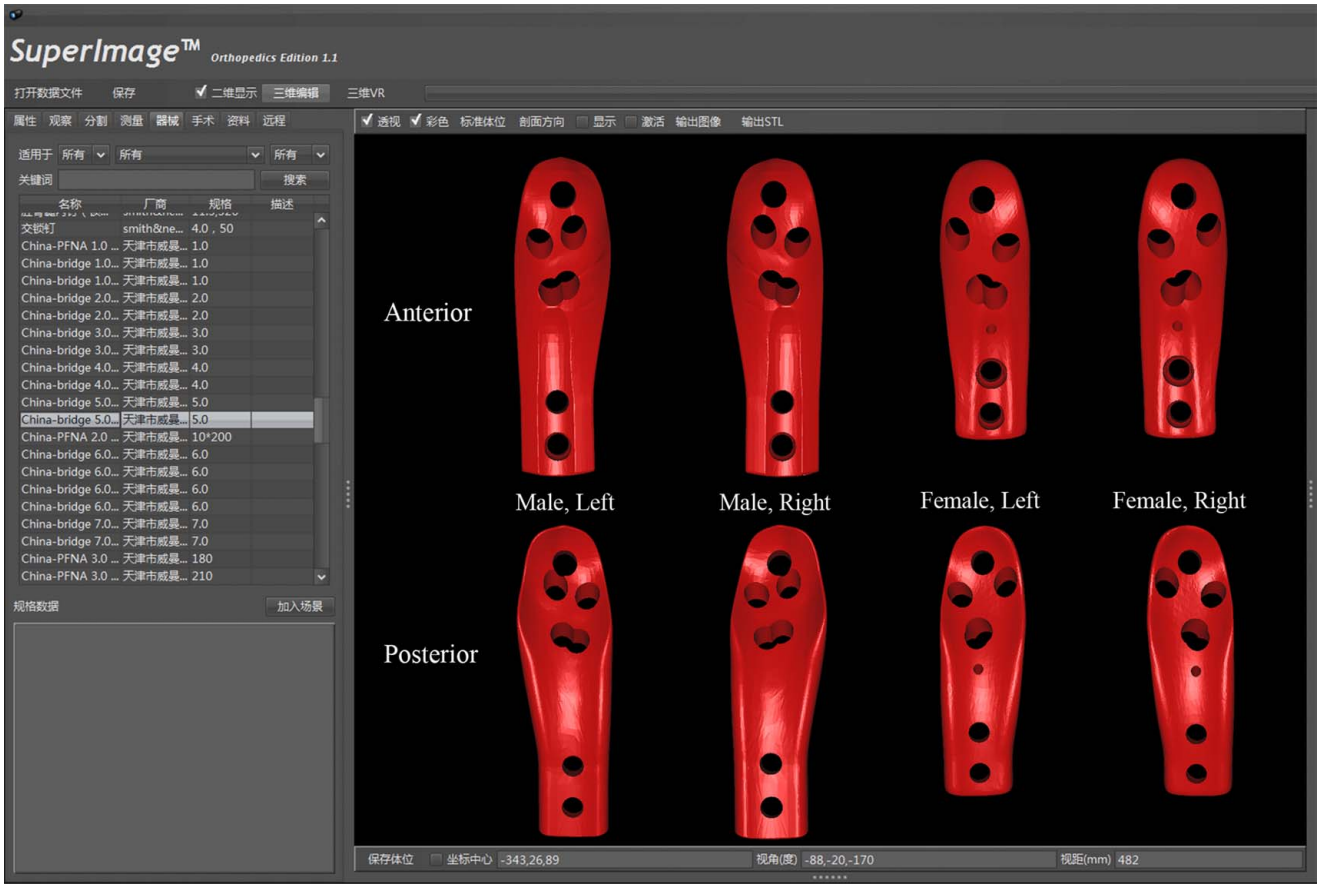

Figure 2. End-structure of anatomical proximal femoral locking plate. End-structure model was divided into male and female version according to the size. The left and right model was mirror structure.

Evaluation of the degree of match of the end-structure

Matching was evaluated by two orthopedists. Each orthopedist assessed the degree of match in a blinded and randomized manner. If the match was less than 80%, the shape of the end-structure needed to be improved on until the match was greater than or equal to 80%. Two weeks after achieving a satisfactory match ($\geq$80%), the match degree of the last end-structure version was re-evaluated for intra-observer analysis.

Verifying reliability of matching evaluation using a 3D printed-model

A certain number of femurs were randomly selected in the matched and unmatched groups, which was derived from data from the first evaluation of the last end-structure version by Orthopedist 1. CT scans of the femurs and end-structures were transferred to a 3D printer (JGAurora Z-603S; JGAurora Technology). Life-sized 3D models of the femurs and end-structures were obtained. The matching evaluation based on the 3D printed models was regarded as the gold standard for assessing the reliability of the matching results based on computer-assisted virtual technology.

Statistical analysis

All parameters were examined for normality using the Kolmogorov–Smirnov test. Quantitative variables are expressed as means with SD or medians and interquartile ranges. The categorical variables are presented as frequencies and percentages.

Sex and side differences in parameters were compared using an independent-sample *t*-test or Mann–Whitney *U*-test. Multireader kappa (κ) statistics were used to estimate the inter- and intra-observer agreements of the matching degree. A value of 0.01–0.20 indicated slight agreement, 0.21–0.40 fair agreement, 0.41–0.60 moderate agreement, 0.61–0.80 substantial agreement, and 0.81–0.99 almost perfect agreement. Additionally, zero indicated no agreement, – 1.00 indicated total disagreement, and + 1.00 indicated perfect agreement[25].

An overall *P*-value of less than 0.05 on two-sides was considered statistically significant. All statistical analyses were performed using SAS (version 9.4; SAS Institute Inc.). The analyses were performed by an independent statistician who was not involved in matching evaluation.

Sample size estimation

Power analysis of the matched proportion

A sample size of 1329 would achieve approximately 80% power to detect a superiority proportion (P0) of 80%, using a one-sided binomial test for superiority, with a nominal significance level of 0.025 and an expected actual proportion (P1) of 83%[26].

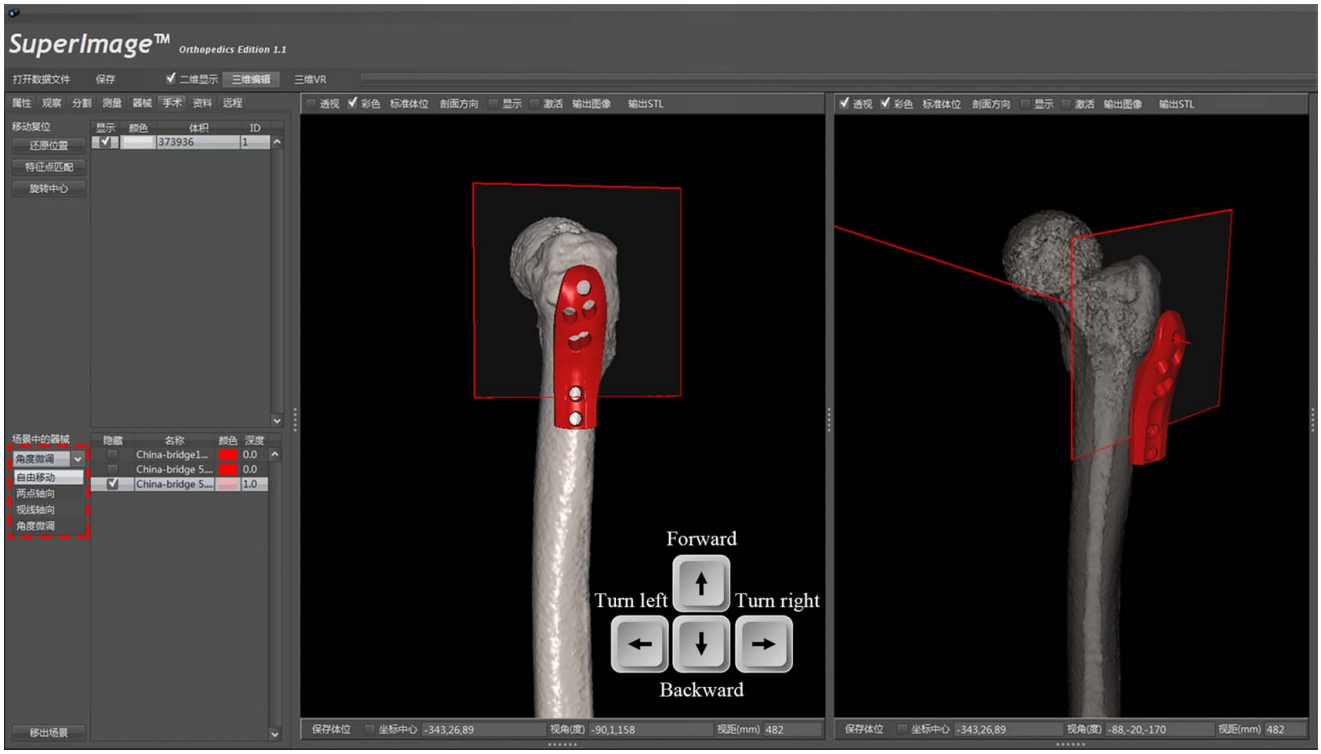

Figure 3. Example of intelligent recognition, fusion, and registration technique for end-structure and bone image. End-structure entered the window point-to-point according to the central position to be placed on the proximal lateral wall of the femur. End-structure could be adjusted in three-dimensions and six degrees of freedom, including forward movement, backward movement, and clockwise and counterclockwise rotation with the center point as the center of the circle.

Considering an attrition rate of ~15%, the total planned sample size was 1600.

Power analysis of the accuracy of the virtual model matching assessment

A sample of 46 each from the matched and unmatched groups would achieve 80% power to detect a difference of 0.150 between the area under the ROC curve under the null hypothesis of 0.700 and that under the alternative hypothesis of 0.850, using a two-sided *Z*-test at a significance level of 0.05[27]. Considering an attrition rate of ~10%, the planned total sample size was 100 (50 matched and 50 unmatched).

Results

Patient characteristics

Of the 1773 patients, 101 (5.7%) were excluded based on one or more of the exclusion criteria. The final study of 1672 patients included 701 (41.9%) men (mean age, 47.2 ± 5.8 years; range, 18–81 years) and 971 (58.1%) women (mean age, 49.4 ± 6.0 years; range, 18–78 years). There were 864 (51.7%) left femurs and 808 (48.3%) right femurs.

Anatomical parameters of the femur

The length of the long axis of the femoral neck averaged 95.2 ± 7.5 mm. The average neck-shaft angle and femoral neck anteversion were 130.6° ± 5.4° and 12.8° ± 4.2°, respectively. The average height and width of the lateral femoral wall was 15.8 ± 3.6 mm and 25.2 ± 2.5 mm, respectively. The superior radius of the anterior, middle, and posterior sections of the lateral wall was 14.2 ± 2.6 mm, 12.8 ± 2.2 mm, and 20.7 ± 3.0 mm, respectively. The inferior radius of the anterior, middle, and posterior sections of the lateral wall was 35.3 ± 4.3 mm, 56.0 ± 6.0 mm, and 90.6 ± 9.3 mm, respectively. The radian of the lateral femoral wall was 20.3 ± 2.6 mm. Significant differences were observed between males and females for all the above parameters (all $P < 0.001$) (Table 1). However, there was no significant difference in the parameters between the left and right sides (Table 1).

Matching degree

In the first version of the end-structure model, the total match rate was 75.0% (526/701 patients) for males and 76.9% (747/971 patients) for females (Table 2). After improving the end-structure model, the total match rate based on orthopedist 1's first evaluation increased to 91.0% (638/701 patients) for males and 92.2% (895/971 patients) for females (Table 3). Similar results were observed in the first evaluation by orthopedist 2 and the second evaluation by both orthopedists (STable 1, Supplemental Digital Content 2, http://links.lww.com/JS9/A246, 2, Supplemental Digital Content 2, http://links.lww.com/JS9/A246, and 3, Supplemental Digital Content 2, http://links.lww.com/JS9/A246).

Inter- and intra-observer reliability

Inter-observer agreement was almost perfect in the first (mean $\kappa = 0.841$ for males; mean $\kappa = 0.865$ for females) and second

Figure 4. Six gaps between the end-structure and plate were identified as indicators and were measured. If the gap was less than or equal to 2 mm, it was allotted 1 point. A total score of greater than or equal to 4 was considered a good match. (A) Anterior, superior arc (gap 1), and inferior arc (gap 2) of the lateral femoral wall. (B) Posterior, superior arc (gap 3), and inferior arc (gap 4) of the lateral femoral wall. (C) Proximal end (gap 5). (D) Distal end (gap 6).

(mean $\kappa = 0.943$ for male; mean $\kappa = 0.862$ for female) evaluations (Table 4). The intra-observer agreement was almost perfect for orthopedist 1 (mean $\kappa = 0.828$ for males; mean $\kappa = 0.891$ for females) and orthopedist 2 (mean $\kappa = 0.935$ for males; mean $\kappa = 0.912$ for females) (Table 5).

Reliability of matching evaluation

The sensitivity and specificity of the matching evaluation based on the computer-assisted virtual model were 96.1% (49/51) and 98.0% (48/49), respectively (Table 6). The percentage of correct interpretations was 97.0% (97/100) (Table 6). The sensitivity, specificity, and percentage of correct interpretations in the male and female models are shown in Table 6.

Discussion

This study showed that a highly matching end-structure of the anatomical proximal femoral locking plate for the Chinese population can be designed using computer-assisted imaging technology and based on a large sample of femoral anatomical parameters. Meanwhile, the efficient and economical process for designing internal fixation systems, which has been described in this study, is valuable for future studies.

Accurate anatomical parameters of the femur are important for designing internal fixation systems. At present, the design of mainstream internal fixation devices was mostly based on the anatomical parameters of the Western populations[17–19,23]. Asian populations have significantly different osseous anatomy compared to Western populations, which could be the main reason for the plate and femur mismatch[14,19,23]. Therefore, it is necessary to accurately measure the femoral anatomical parameters of the Chinese population and design a suitable internal fixation system. However, the femoral anatomical structure of the Chinese population has not been extensively studied. Moreover, the femoral anatomical parameters have been previously measured in cadavers and on radiographs or conventional CT[13,23,28], which have their own limitations. First, it was difficult to obtain cadaver specimens and carry out large sample-sized prospective studies. Radiographs may be limited by the position of the patient's limbs. Finally, the selection of axial CT images may be affected by the position of the limb and the reconstruction interval. In the current study, anatomical parameters of the proximal femur in

Table 1

Anatomical parameters of proximal femur*

Parameters	Total ($n=1672$)	Sex				Side			
		Male ($n=701$)	Female ($n=971$)	Mean difference	*P*	Left ($n=864$)	Right ($n=808$)	Mean difference	*P*
Length of long axis of femoral neck (mm)	95.2 (7.5)	97.1 (7.9)	93.9 (7.0)	3.2 (2.4–3.9)	< 0.001	95.1 (7.6)	95.4 (7.5)	– 0.3 (– 1.0–0.4)	0.40
Neck-shaft angel (°)	130.6 (5.4)	129.1 (5.2)	131.7 (5.2)	– 2.56 (– 3.1 to – 2.1)	< 0.001	130.8 (5.6)	130.3 (5.1)	0.5 (– 0.003–1.0)	0.05
Anteversion of femoral neck (°)	12.8 (4.2)	10.5 (3.5)	14.5 (3.9)	– 3.9 (– 4.3 to – 3.6)	< 0.001	12.9 (4.1)	12.7 (4.3)	0.2 (– 0.3–0.6)	0.47
Height of lateral wall (mm)	15.8 (3.6)	17.7 (3.0)	14.4 (3.4)	3.3 (3.0– 3.6)	< 0.001	15.9 (3.6)	15.7 (3.7)	0.2 (– 0.2–0.5)	0.39
Width of lateral wall (mm)	25.2 (2.5)	27.5 (1.7)	23.5 (1.4)	4.0 (3.9–4.2)	< 0.001	25.2 (2.5)	25.2 (2.5)	– 0.009 (– 0.3–0.2)	0.94
Superior radius (mm)									
Anterior	14.2 (2.6)	16.5 (1.9)	12.5 (1.4)	4.1 (3.9–4.2)	< 0.001	14.2 (2.6)	14.2 (2.6)	– 0.05 (– 0.3–0.2)	0.72
Middle	12.8 (2.2)	14.4 (1.9)	11.5 (1.5)	3.0 (2.8–3.1)	< 0.001	12.8 (2.2)	12.8 (2.2)	– 0.002 (– 0.2–0.2)	0.99
Posterior	20.7 (3.0)	22.4 (3.0)	19.4 (2.2)	3.0 (2.8–3.3)	< 0.001	20.6 (3.0)	20.8 (2.9)	– 0.1 (– 0.4–0.2)	0.40
Inferior radius (mm)									
Anterior	35.3 (4.3)	36.6 (4.4)	34.3 (4.0)	2.3 (1.9–2.7)	< 0.001	35.3 (4.2)	35.2 (4.5)	0.2 (– 0.2–0.6)	0.40
Middle	56.0 (6.0)	57.6 (7.0)	54.8 (5.0)	2.8 (2.2–3.4)	< 0.001	56.3 (5.9)	55.6 (6.2)	0.7 (0.1–1.3)	0.02
Posterior	90.6 (9.3)	92.0 (10.3)	89.6 (8.4)	2.3 (1.4–3.2)	< 0.001	90.7 (9.6)	90.5 (9.0)	0.2 (– 0.7–1.1)	0.66
Radian of lateral wall (mm)	20.3 (2.6)	21.2 (3.0)	19.6 (2.0)	1.7 (1.4–1.9)	< 0.001	20.3 (2.6)	20.3 (2.6)	– 0.05 (– 0.3–0.2)	0.72

P values are based on independent-sample *t*-test or Mann–Whitney *U* test.

*Normally distributed data are presented as mean (standard deviation) and data that are not normally distributed are presented as medians (ranges or interquartile ranges).

Table 2

Matching rate of end-structure of anatomical proximal femoral locking plate before modification.

	Male			Female		
	Total ($n=701$)	Left ($n=358$)	Right ($n=343$)	Total ($n=971$)	Left ($n=506$)	Right ($n=465$)
Matched	526 (75.0%)	269 (75.1%)	257 (74.9%)	747 (76.9%)	391 (77.3%)	356 (76.6%)
Unmatched	175 (25.0%)	89 (24.9%)	86 (25.1%)	224 (23.1%)	115 (22.7%)	109 (23.4%)

Data are presented as number (percentage).

Table 3

Matching rate of end-structure of anatomical proximal femoral locking plate after modification at first evaluation of orthopedist 1.

	Male			Female		
	Total ($n=701$)	Left ($n=358$)	Right ($n=343$)	Total ($n=971$)	Left ($n=506$)	Right ($n=465$)
Matched	638 (91.0%)	330 (92.2%)	308 (89.8%)	895 (92.2%)	455 (89.9%)	440 (94.6%)
Unmatched	63 (9.0%)	28 (7.8%)	35 (10.2%)	76 (7.8%)	51 (10.1%)	25 (5.4%)

Data are presented as number (percentage).

Table 4

Interobserver agreement on matching of end-structure of anatomical proximal femoral locking plate.

	Orthopedist 2							
	Male				Female			
	First evaluation		Second evaluation		First evaluation		Second evaluation	
Orthopedist 1	Matched	Unmatched	Matched	Unmatched	Matched	Unmatched	Matched	Unmatched
First evaluation								
Matched	630*	8	NA	NA	890*	5	NA	NA
Unmatched	10	53*	NA	NA	13	63*	NA	NA
Second evaluation								
Matched	NA	NA	641*	2	NA	NA	892*	6
Unmatched	NA	NA	4	54*	NA	NA	12	61*

*Data are number of agreements.
NA indicate not appliable.

Chinese individuals were accurately measured using 3D CT images. Furthermore, the CT images were obtained from a large sample, which was a good representation of the population. Similar to that in previous studies, there were significant differences in the anatomical parameters of the proximal femur between the men and women in our study[13,29]. Therefore, two sets of end-structure models were designed according to sex. No significant difference was observed in the anatomical parameters between the left and right sides. Thus, when designing the left and right end-structures, mirror image processing alone was adequate.

To evaluate and verify the agreement of matching between the bone and end-structure based on the computer-assisted virtual reconstruction, two orthopedists conducted two evaluations; the inter- and intra-observer agreements were also calculated. Almost perfect agreement was achieved in the study (Fig. 5). Thereafter, 100 3D models of the femur and end-structure were printed as the gold standard to verify the reliability of evaluating structural matching virtually. Satisfactory sensitivity, specificity, and percentage of correct interpretations were observed in the virtual mode (Fig. 6).

The methodology used for measuring parameters in this study was scientific and reliable, which has been proven by previous studies[30,31]. In addition, the end-structure design process was economical and efficient. Virtual reconstruction and matching were performed using a computer-aided orthopedic clinical research platform developed by our research team. Therefore, no additional costs were incurred. Certain additional costs were incurred in the 3D printing process. However, to ensure the statistical power, a certain number of models were randomly selected for printing, which allowed some control of the cost. The process from femur reconstruction to completion of internal fixation matching took ~3 min. Moreover, reconstruction, measurement, and matching were all completed in one system.

This study had some limitations. First, the included patients were not randomly selected from the overall social population, which could have led to some selection bias. However, this was considered during the study-design stage, and the minimum sample size was determined using a power analysis. The current study included a larger sample size than the calculated minimum size, making the study highly reliable. However, random sampling based on a larger sample population is required in future studies. Second, end-structure of the proximal femoral plate was not biomechanically evaluated. Biomechanical evaluation of internal fixation systems, including that of cadaveric and finite element computational biomechanics[32,33], is an important and indispensable process before clinical application. However, the postproduction end-structure of this study used special metal materials and corresponding thicknesses that have been widely used in clinical practice, and the main purpose of this study was to design a well-matched end-structure of the proximal femoral

Table 5

Intraobserver agreement on matching of end-structure of anatomical proximal femoral locking plate.

	Second evaluation							
	Male				Female			
	Orthopedist 1		Orthopedist 2		Orthopedist 1		Orthopedist 2	
First evaluation	Matched	Unmatched	Matched	Unmatched	Matched	Unmatched	Matched	Unmatched
Orthopedist 1								
Matched	631*	7	NA	NA	889*	6	NA	NA
Unmatched	12	51*	NA	NA	9	67*	NA	NA
Orthopedist 2								
Matched	NA	NA	639*	1	NA	NA	898*	5
Unmatched	NA	NA	6	55*	NA	NA	6	62*

*Data are number of agreements.
NA indicate not appliable.

Table 6

Assessment of the accuracy of the end-structure matching evaluation based on computer-assisted virtual technology.

	Ture result (3D printing)			Ture result (3D printing)				
				Male		Female		
Computer-assisted	Matched	Unmatched	Total	Matched	Unmatched	Matched	Unmatched	Total
Matched	49*	1	50	26*	1	23*	0	50
Unmatched	2	48†	50	1	23†	1	25†	50
Total	51	49	100	27	24	24	25	100

*Data are used to calculate sensitivity.
†Data are used to calculate specificity.

plate. In addition, the end-structure will be biomechanically evaluated in our subsequent studies. Third, some people may argue that the degree of match between the end-structure and proximal femur was evaluated on computer-assisted 3D images and not on actual clinical patients, which might affect its clinical application. However, this concern may be allayed for the following reasons: no significant difference has been reported in the measurement of bone morphology parameters between 3D images and real bones[34]; the sample size of this study was relatively large and was representative of the population; and good reliability of the end-structure matching was demonstrated using 3D printed models. No significant difference has been reported in the morphological parameters between 1:1 3D printed models and real bones[35,36]. Evaluation of the clinical efficacy of the end-structure will be the focus of our future studies.

Conclusion

This study accurately measured the anatomical parameters of the proximal femur in a large sample of the Chinese population. An end-structure of the proximal femoral locking plate was designed in line with the measured skeletal morphological characteristics.

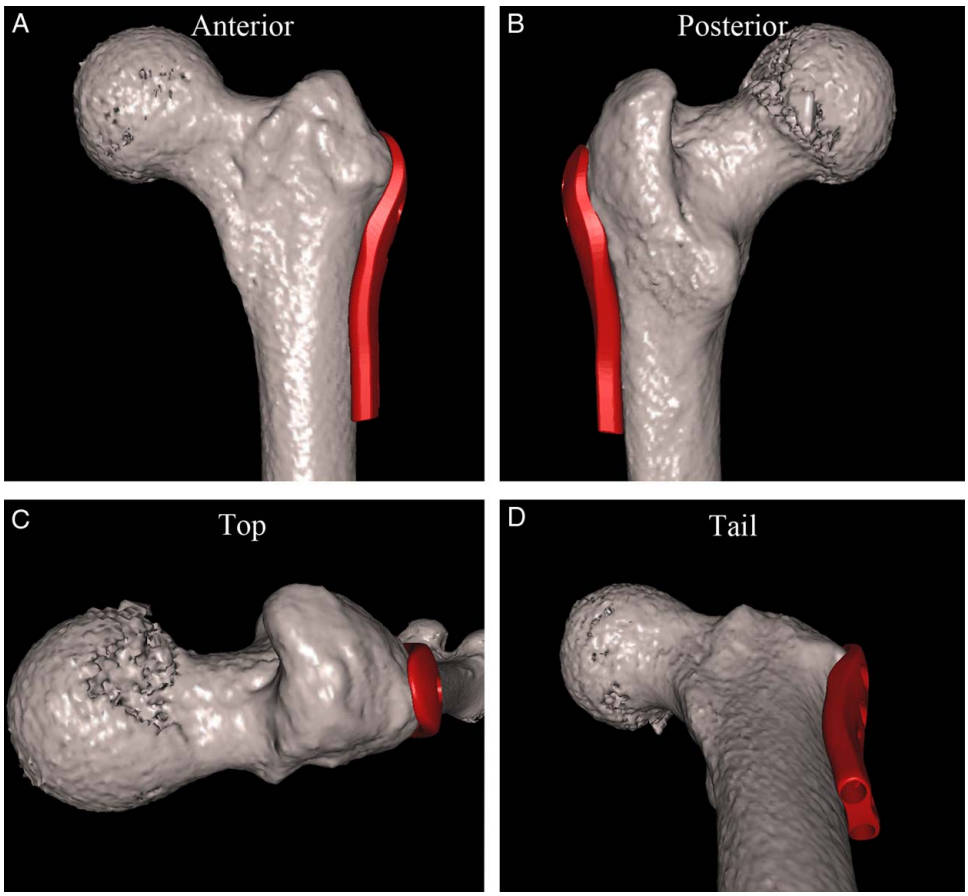

Figure 5. Good match was achieved between proximal femur and end-structure that was designed based on large samples of anatomical parameters of femur on the Chinese population. From anterior (A), posterior (B), proximal end (C), and distal end (D) directions, there were no obvious gap between end-structure and proximal femur.

Figure 6. End-structure of anatomical proximal femoral locking plate of three-dimensional printing (A and B) and titanium alloy (C and D). Good match was achieved between proximal femur and end-structure in three-dimensional printing model (E, F, G, and H) and titanium alloy model (I, J, K, and L).

Additionally, this study employed an innovative process for designing internal fixation systems. This process verified the matching of large samples of bones and internal fixation systems in a relatively short time in an economical and efficient manner. Additionally, it determined a design that conformed to the anatomical shape of bone to the maximum extent. The methodology described in this study will be a valuable reference for future studies.

Ethical approval

The study was approved by our Institutional Review Board of East Hospital, Tongji University School of Medicine and was in compliance with the Declaration of Helsinki.

Sources of funding

This study was supported by the National Natural Science Foundation of China (No. 82272479).

Author contribution

X.Y.J.: conceptualization, methodology, formal analysis, writing-original draft; K.Z.: conceptualization, methodology, writing-original draft; M.F.Q.: software, validation, resources; Q.H.H.: software, investigation, data curation, visualization; G.J.Z.: software, visualization; Y.W.: conceptualization, methodology, formal analysis, visualization; Y.X.C.: conceptualization, methodology, visualization, resources, supervision.

Conflicts of interest disclosure

The authors declare that they have no financial conflict of interest with regard to the content of this report.

Research registration unique identifying number (UIN)

1. Name of the registry: Research Registry.

2. Unique Identifying number or registration ID: researchregistry8413
3. Hyperlink to your specific registration (must be publicly accessible and will be checked): https://www.researchregistry.com/browse-theregistry#home/registrationdetails/634e78d9a784f6002118a7bc/

Guarantor

Yanxi Chen.

Data statement

The data that support the findings of this study are available on reasonable request from the corresponding author. The data are not publicly available due to privacy and ethical restrictions.

Provenance and peer review

Not commissioned, externally peer-reviewed.

References

[1] Yang G, Wang Y, Zeng Y, *et al*. Rapid health transition in China, 1990-2010: findings from the Global Burden of Disease Study 2010. Lancet 2013;381:1987–2015.
[2] Wang SY, Li YH, Chi GB, *et al*. Injury-related fatalities in China: an under-recognised public-health problem. Lancet 2008;372:1765–73.
[3] Cooper C, Campion G, Melton LJ III. Hip fractures in the elderly: a world-wide projection. Osteoporos Int 1992;2:285–9.
[4] Soliman G, Fortinsky RH, Mangione K, *et al*. Impact of psychological resilience on walking capacity in older adults following hip fracture. J Am Geriatr Soc 2022;70:3087–95.
[5] Vigni GE, Bosco F, Cioffi A, *et al*. Mortality risk assessment at the admission in patient with proximal femur fractures: electrolytes and renal function. Geriatr Orthop Surg Rehabil 2021;12:21514593219915O3.
[6] Bosco F, Vittori J, Grosso E, *et al*. Contralateral non-simultaneous proximal femoral fractures in patients over 65 years old. Eur J Orthop Surg Traumatol 2022;32:71–9.
[7] Dare AJ, Hu G. China's evolving fracture burden. Lancet Glob Health 2017;5:e736–7.
[8] Bhandari M, Swiontkowski M. Management of acute hip fracture. N Engl J Med 2017;377:2053–62.
[9] Brox WT, Roberts KC, Taksali S, *et al*. The American academy of orthopaedic surgeons evidence-based guideline on management of hip fractures in the elderly. J Bone Joint Surg Am 2015;97:1196–9.
[10] Roberts KC, Brox WT. From evidence to application: AAOS clinical practice guideline on management of hip fractures in the elderly. J Orthop Trauma 2015;29:119–20.
[11] Roberts KC, Brox WT, Jevsevar DS, *et al*. Management of hip fractures in the elderly. J Am Acad Orthop Surg 2015;23:131–7.
[12] Bottlang M, Lesser M, Koerber J, *et al*. Far cortical locking can improve healing of fractures stabilized with locking plates. J Bone Joint Surg Am 2010;92:1652–60.
[13] Lin KJ, Wei HW, Lin KP, *et al*. Proximal femoral morphology and the relevance to design of anatomically precontoured plates: a study of the Chinese population. ScientificWorldJournal 2014;2014:106941.
[14] Schmutz B, Kmiec S Jr, Wullschleger ME, *et al*. 3D Computer graphical anatomy study of the femur: a basis for a new nail design. Arch Orthop Trauma Surg 2017;137:321–31.
[15] Thiesen DM, Ntalos D, Korthaus A, *et al*. A comparison between Asians and Caucasians in the dimensions of the femoral isthmus based on a 3D-CT analysis of 1189 adult femurs. Eur J Trauma Emerg Surg 2022;48:2379–86.
[16] Khalafi A, Curtiss S, Hazelwood S, *et al*. The effect of plate rotation on the stiffness of femoral LISS: a mechanical study. J Orthop Trauma 2006;20:542–6.
[17] Ji JH, Jeong JY, Song HS, *et al*. Early clinical results of reverse total shoulder arthroplasty in the Korean population. J Shoulder Elbow Surg 2013;22:1102–7.
[18] Tang Q, Zhou Y, Yang D, *et al*. The offset of the tibial shaft from the tibial plateau in Chinese people. J Bone Joint Surg Am 2010;92:1981–7.
[19] Zhang Q, Shi LL, Ravella KC, *et al*. Distinct proximal humeral geometry in chinese population and clinical relevance. J Bone Joint Surg Am 2016;98:2071–81.
[20] Ogrinc G, Davies L, Goodman D, *et al*. SQUIRE 2.0 (Standards for QUality Improvement Reporting Excellence): revised publication guidelines from a detailed consensus process. BMJ Qual Saf 2016;25:986–92.
[21] Jia X, Zhang K, Qiang M, *et al*. Association of computer-assisted virtual preoperative planning with postoperative mortality and complications in older patients with intertrochanteric hip fracture. JAMA Netw Open 2020;3:e205830.
[22] Jia X, Zhang K, Qiang M, *et al*. The accuracy of intra-operative fluoroscopy in evaluating the reduction quality of intertrochanteric hip fractures. Int Orthop 2020;44:1201–8.
[23] Hoaglund FT, Low WD. Anatomy of the femoral neck and head, with comparative data from Caucasians and Hong Kong Chinese. Clin Orthop Relat Res 1980;152:10–6.
[24] Hu ZS, Liu XL, Zhang YZ. Comparison of proximal femoral geometry and risk factors between femoral neck fractures and femoral intertrochanteric fractures in an elderly chinese population. Chin Med J (Engl) 2018;131:2524–30.
[25] Landis JR, Koch GG. The measurement of observer agreement for categorical data. Biometrics 1977;33:159–74.
[26] Fleiss JL, Levin B, Paik MC. Statistical Methods for Rates and Proportions, Third Edition. John Wiley & Sons; 2003.
[27] Obuchowski NA, McClish DK. Sample size determination for diagnostic accuracy studies involving binormal ROC curve indices. Stat Med 1997;16:1529–42.
[28] Hermann KL, Egund N. CT measurement of anteversion in the femoral neck. The influence of femur positioning. Acta Radiol 1997;38:527–32.
[29] Casper DS, Kim GK, Parvizi J, *et al*. Morphology of the proximal femur differs widely with age and sex: relevance to design and selection of femoral prostheses. J Orthop Res 2012;30:1162–6.
[30] Jia XY, Chen YX, Qiang MF, *et al*. Postoperative evaluation of reduction loss in proximal humeral fractures: a comparison of plain radiographs and computed tomography. Orthop Surg 2017;9:167–73.
[31] Jia X, Chen Y, Qiang M, *et al*. Compared to X-ray, three-dimensional computed tomography measurement is a reproducible radiographic method for normal proximal humerus. J Orthop Surg Res 2016;11:82; 2016.
[32] Chethan KN, Shyamasunder Bhat N, Zuber M, *et al*. Finite element analysis of hip implant with varying in taper neck lengths under static loading conditions. Comput Methods Programs Biomed 2021;208:106273.
[33] Chethan KN, Zuber M, Shyamasunder Bhat N, *et al*. Optimized trapezoidal-shaped hip implant for total hip arthroplasty using finite element analysis. Cogent Engineering 2020;7:1.
[34] Boileau P, Cheval D, Gauci MO, *et al*. Automated three-dimensional measurement of glenoid version, and inclination in arthritic shoulders. J Bone Joint Surg Am 2018;100:57–65.
[35] Beredjiklian PK, Wang M, Lutsky K, *et al*. Three-dimensional printing in orthopaedic surgery: technology and clinical applications. J Bone Joint Surg Am 2020;102:909–19.
[36] Meyer-Szary J, Luis MS, Mikulski S, *et al*. The role of 3d printing in planning complex medical procedures and training of medical professionals-cross-sectional multispecialty review. Int J Environ Res Public Health 2022;19:3331.